Article:
Del Piero, N, Riguad, S, Takahashi, S et al. (2 more authors) (2020) Unravelling the paleoecology of flat clams: new insights from an Upper Triassic halobiid bivalve. Global and Planetary Change, 190. 103195. ISSN 0921-8181

https://doi.org/10.1016/j.gloplacha.2020.103195

Unravelling the paleoecology of flat clams: new insights from an Upper Triassic halobiid bivalve

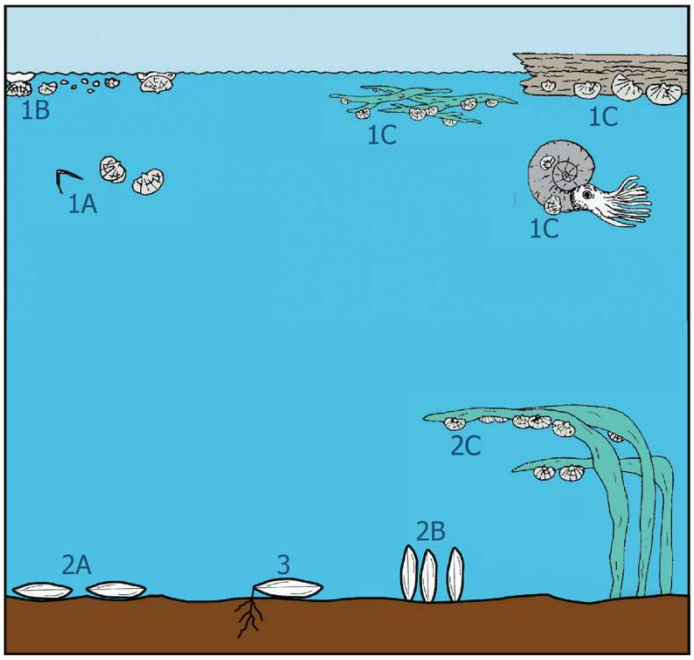

Fig. 1- Reconstruction of proposed modes of life for flat clams. 1A) Nektonic; 1B) Holopelagic; 1C) Pseudoplanktonic; 2A) Epibenthic recliners; 2B) Benthic mudstickers; 2C) Epiphytic; 3) Epibenthic chemosymbionts (modified after Wignall, 1994 and Schatz, 2004).

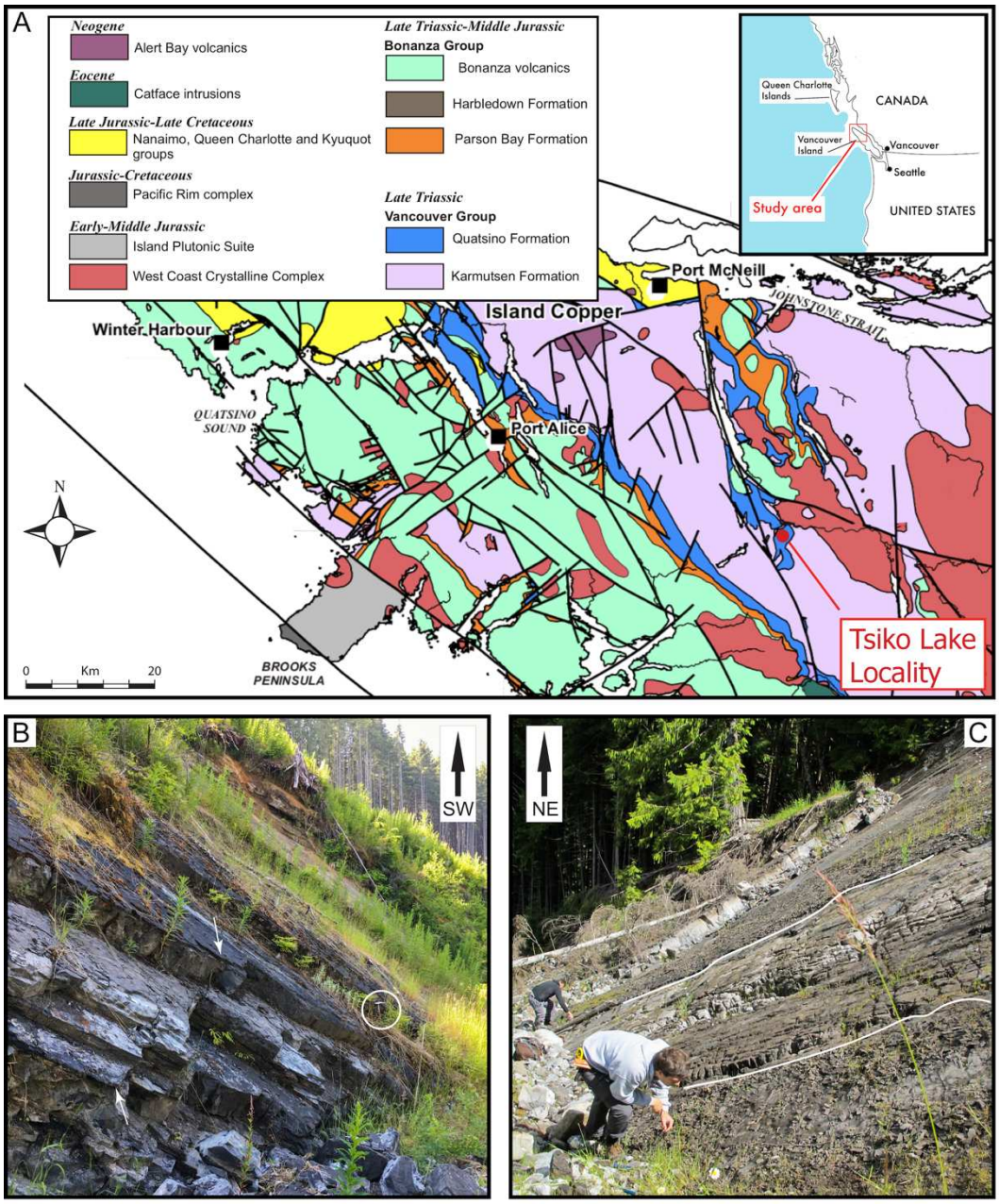

Fig. 2- Introduction to the study area. A) Bedrock geology of Northern Vancouver Island showing the location of Tsiko Lake (modified after Massey et al., 2005 and Nixon et al. 2006); B) Bedding on the lower part of the sequence. White arrows indicate thin-bedded occurrences of bituminous shales (hammer as scale: circle); C) Halobia collection on fissile calcareous siltstone on the upper part of the sequence. White lines delimitate the areas where the bed is still exposed and fossil collection was made; in the central area the bed has been eroded away.

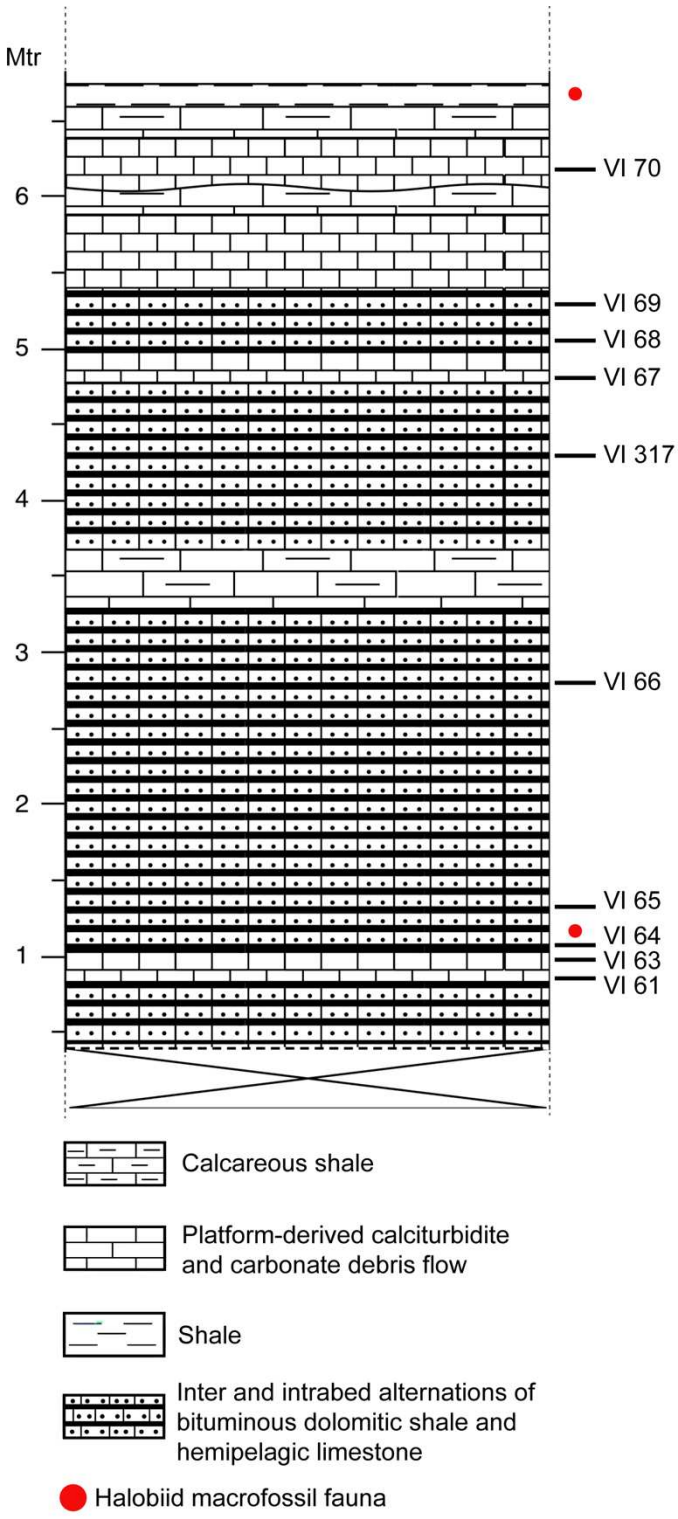

Fig. 3- Stratigraphy, lithology and samples location at Tsiko Lake section.

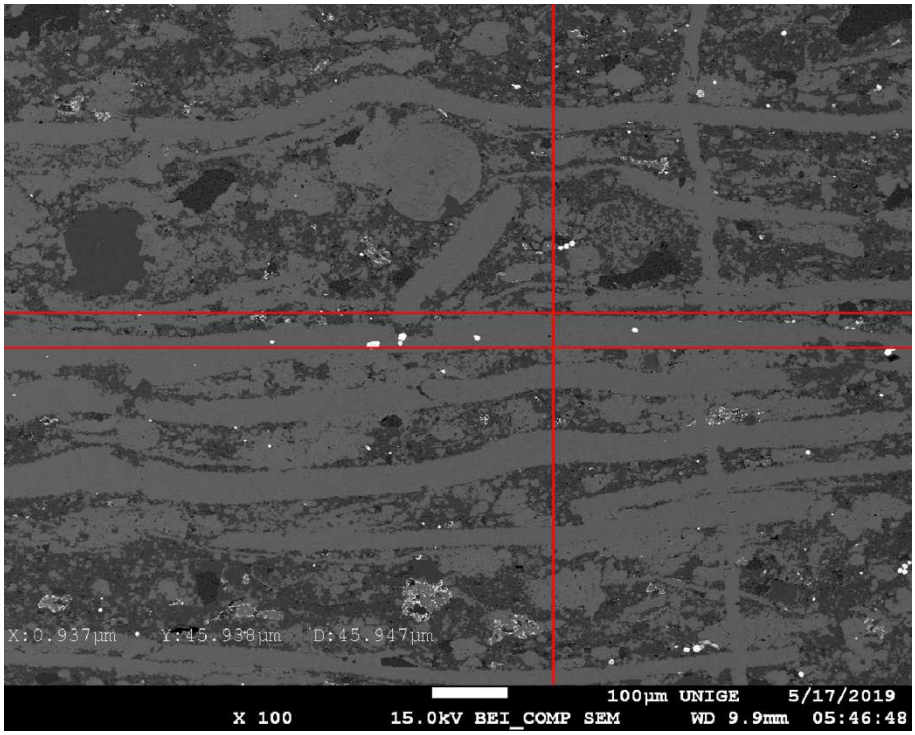

Fig. 4- SEM image of sample VI 69 A from Tsiko Lake taken in BSE mode. Measurements were taken along a fixed vertical line to avoid preferential selection. Bright yellow dots are different forms of pyrite.

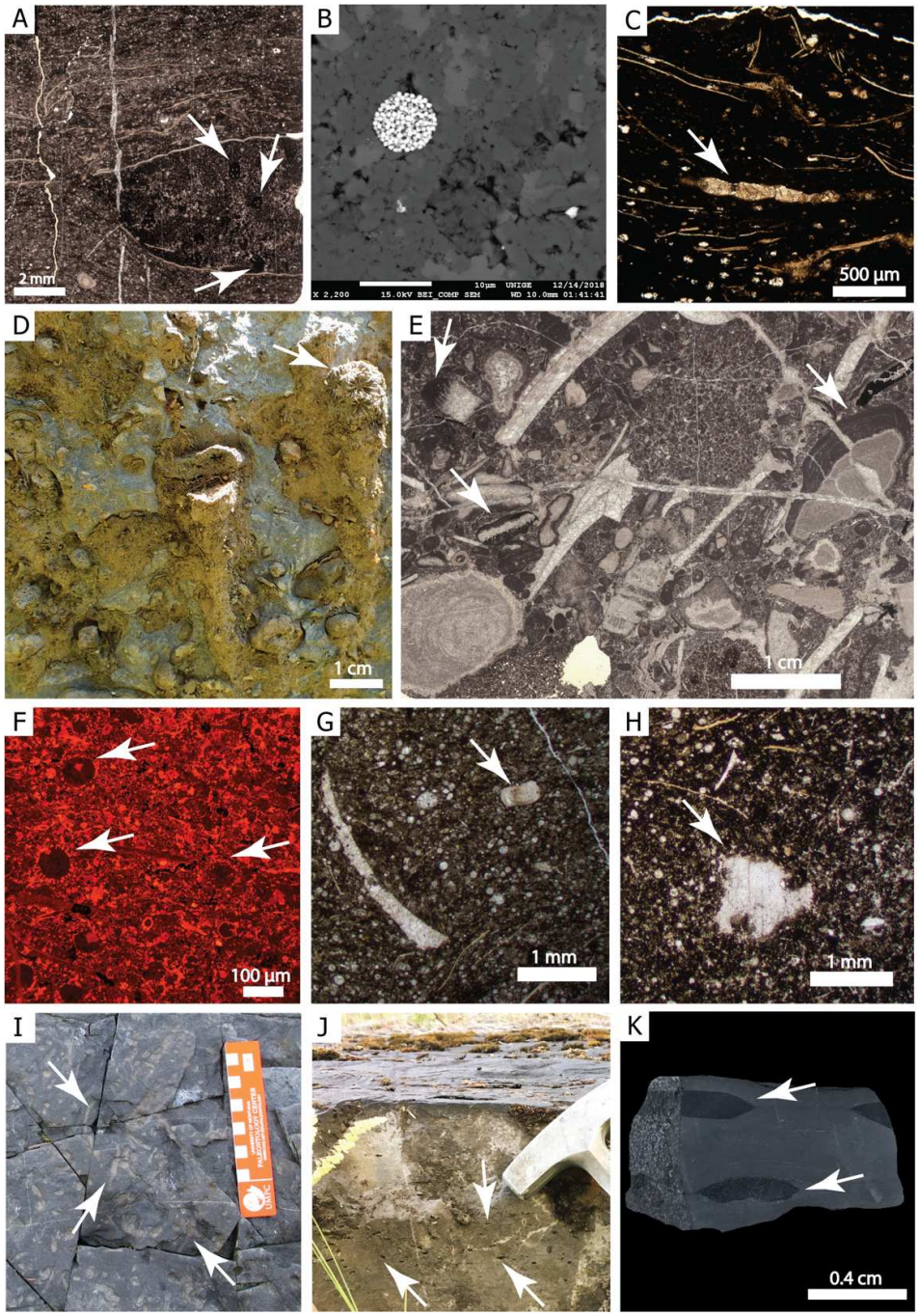

Fig. 5- Thin section, SEM, cathodoluminescence and field photographs of samples from Tsiko Lake. A) Closed articulated *Halobia* in life position showing the more inflated valve at the bottom: note the coprolith-rich infilling of the *Halobia* specimen (white arrows), which differs from the surrounding matrix (sample VI 68 B 2); B) Framboidal pyrite (sample VI 68 B 2); C) Nodosarid foraminifera (white arrow) found in the oxygenation laminae of BFC 3 (sample VI 64 A); D) Macroscopic view of one of the coarse gravitational flows bearing silicified shallow-water fauna: a specimen of coral (white arrow) is easily distinguishable; E) Thin section view of the same sample (VI 70 C): note the thick microbial coating on some of the bioclasts (white arrows); F) Spumellarian radiolarians (white arrows) in BFC 1 (VI 63 B 1); G) Fragment of a bivalve together with a fish otolith (white arrow) in BFC 1 (sample VI 63 B); H) Fragment of a crinoid plate (white arrow) in BFC 1 (sample VI 63 B); I) *Phycosiphon* sp. trace (white arrows) along with other undetermined ichnotaxa on a bedding plane; J) Bioturbation in transversal view (white arrows); K) Flattened *Chondrites* sp. burrows on a hand sample of BFC 3 (sample VI 64 A). Note the bitumen staining in the burrows (white arrows).

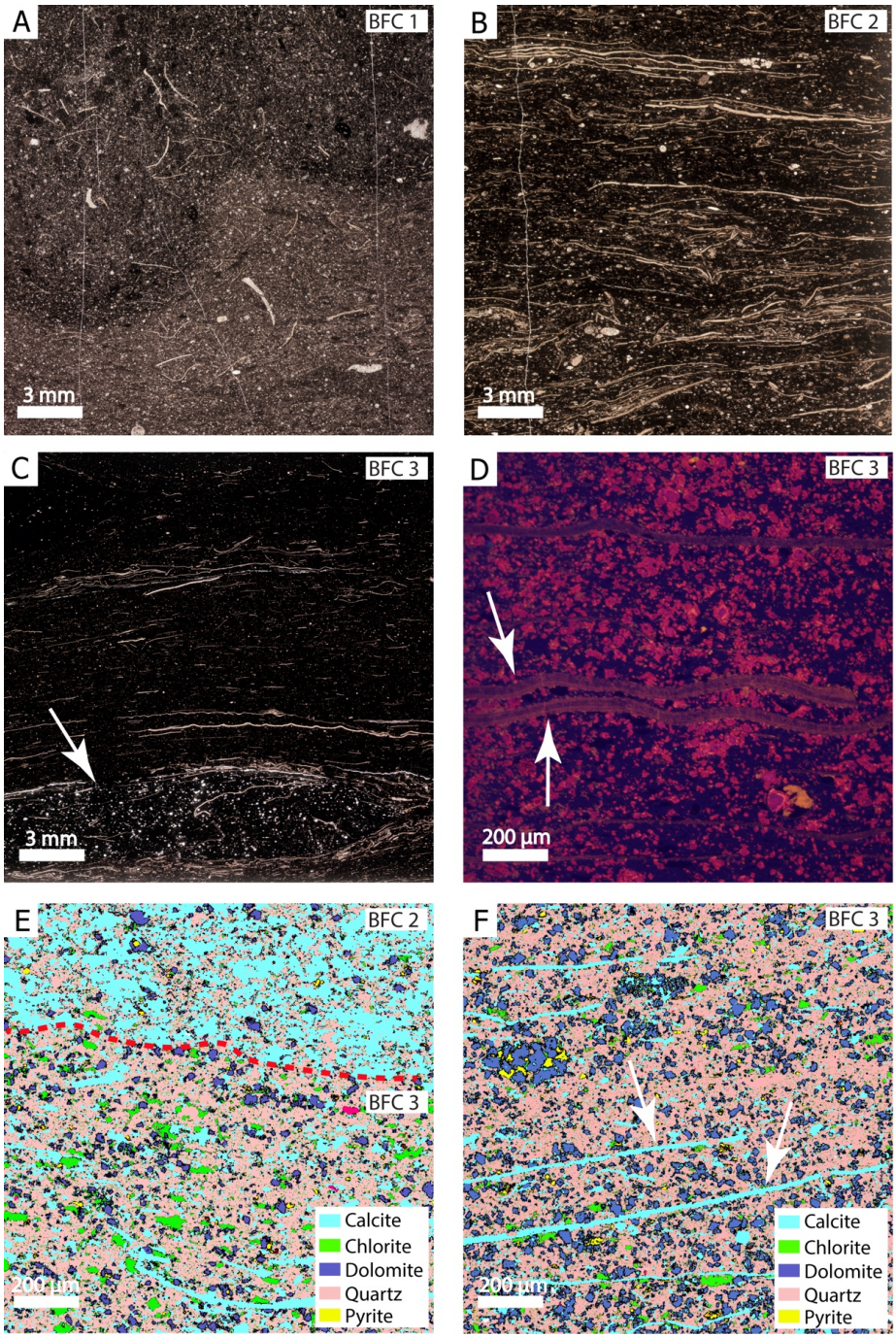

Fig.6- Thin section, cathodoluminescence and QEMSCAN images of samples from Tsiko Lake. A) Moderately bioturbated radiolarian-rich wackestone to packstone of BFC 1 (sample VI 63 B); B) *Halobia*-rich floatstone with wackestone matrix of BFC 2 (sample VI 69 A); C) Wavy-laminated wackestone to floatstone with wackestone matrix of BFC 3 (sample VI 64 A): in the bottom part of the picture you can see one of these areas burrowed by *Chondrites* sp. (white arrow): the burrowing comes along with thicker halobiids and small benthic foraminifera (sample VI 64 A); D) Cathodoluminescence image of BFC 3: note that the layering inside *Halobia* shells is still preserved (white arrows; sample VI 64 B). Three-phases zonation of dolomite is also clearly visible; E) QEMSCAN image showing the transition between BFC 2 (sample VI 65 C) and BFC 3 (sample VI 65 B) (red dashed line). Generally, BFC 3 received les biogenic input along with more clastic material. Dolomite is more present in organic-rich BFC 3; F) QEMSCAN image of BFC 3 showing small *Halobia* (white arrows) now preserved with calcite mineralogy (sample VI 64 A).

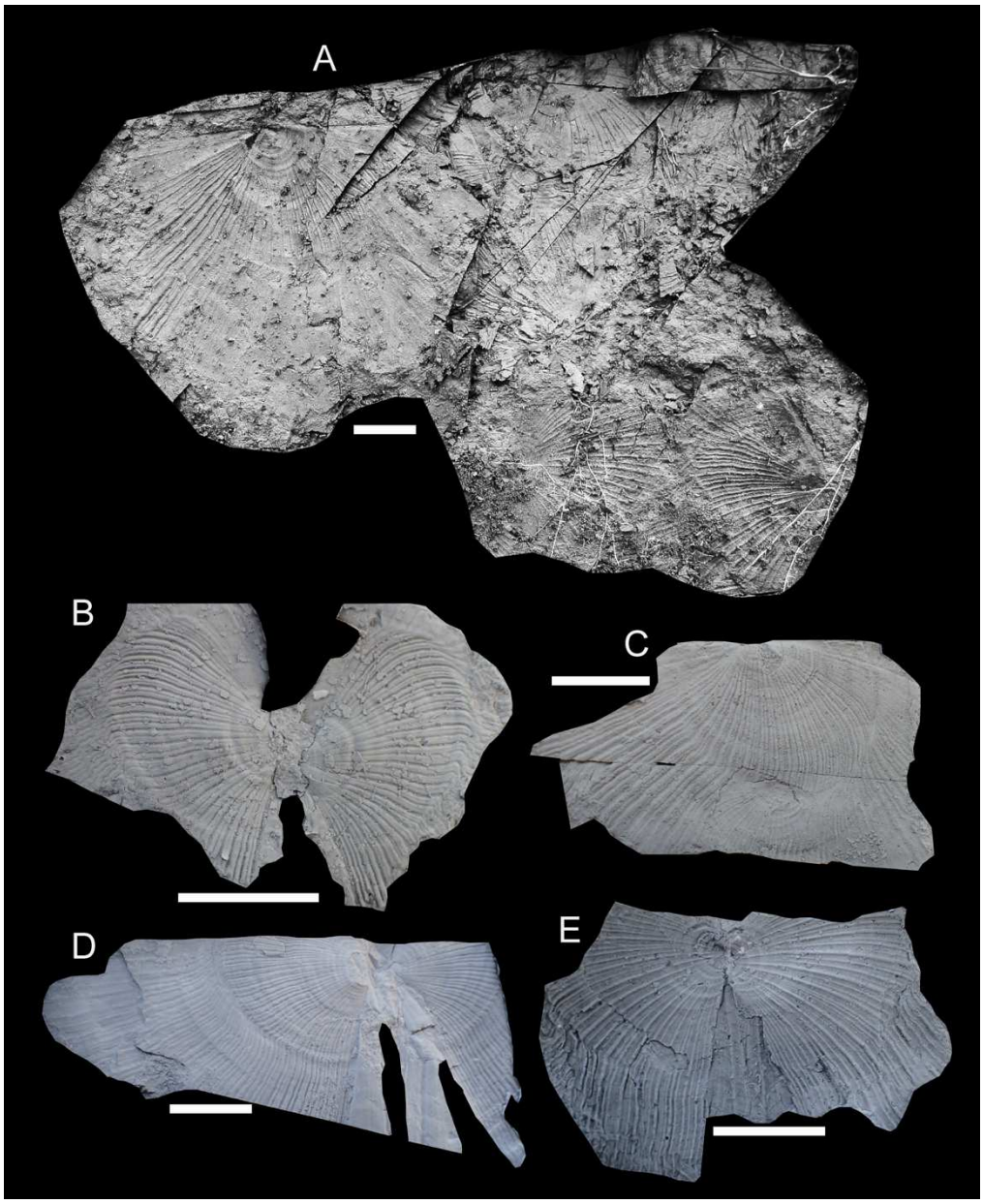

Fig. 7- Some of the *Halobia* specimens examined in this study. A) *Halobia* occurrences on the bedding plane on top of the section (upper red dot), note the generally unfragmented nature of the shells; B-E) Specimens of *Halobia Cordillerana* Smith, 1927. Most of these halobiids have been found with open articulated preservation (B-D-E). Scale bar is 1 cm; B= sample TL (Tsiko Lake) 1.21, C= sample TL 1.22, D= sample TS 1.15, E= sample TS 1.27.

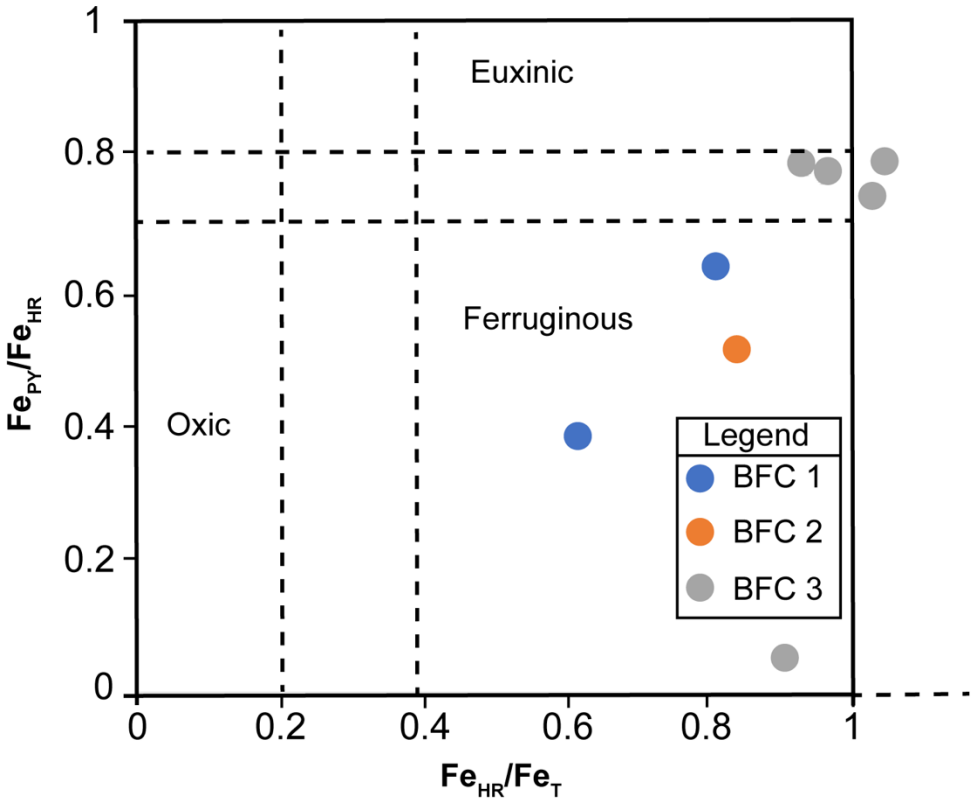

Fig. 8- Plot showing the Fe distribution in the three biofacies. Limit among the different depositional conditions are set according to what is mentioned in the text. Generally, a gradual enrichment both in Fe_{HR} and Fe_{PY} is seen from BFC 1 to BFC 2 and BFC 3. The BFC 3 sample on the lower bottom represents VI 317 A which underwent oxidative weathering as discussed in the text.

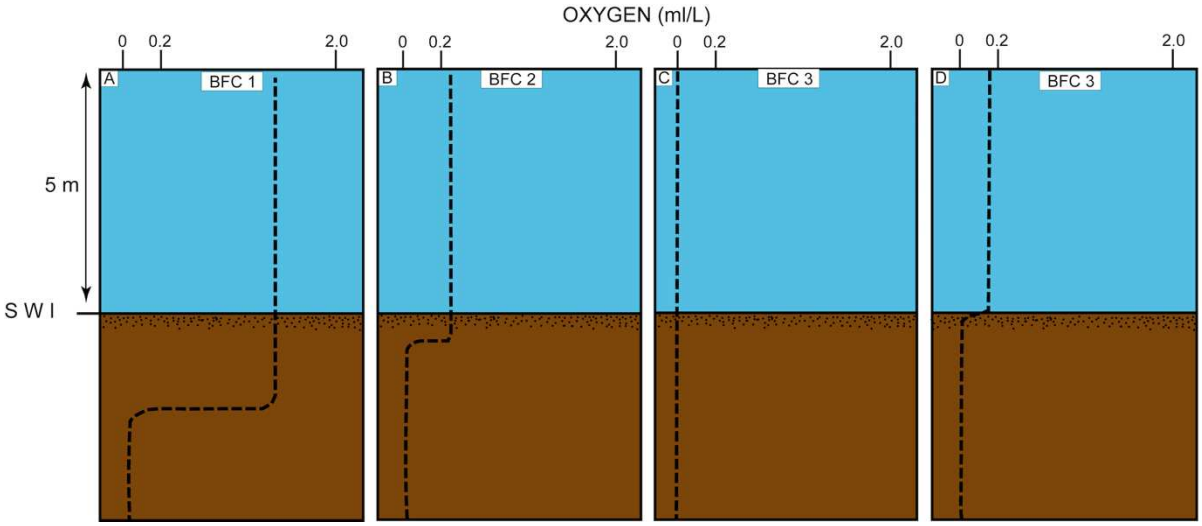

Fig. 9- Interpretation of the oxygen conditions on the sea bottom at the time of deposition for the three different biofacies (modified from Savrda and Bottjer, 1991). Absolute oxygen values are taken from Tyson and Pearson (1991): D.O. (dissolved oxygen) > 2 ml/L =oxic, 2 < D.O. > 0.2 = dysoxic, 0.2 < D.O. > 0.0 =suboxic, D.O. = 0.0 ml/L =anoxic. A) Oxygen profile during the deposition of BFC 1: the chemocline is located well below the sediment water interface (SWI); B) Oxygen profile during the deposition of BFC 2: in this case the chemocline [or RPD (redox potential discontinuity) as defined by Rhoads and Morse (1971)] is located inside the sediment at shallower depth if compared to BFC 1; C) Oxygen profile during the anoxic/euxinic periods of BFC 3: in this case the chemocline was located in the water column; D) Oxygen profile during the oxygenation events in BFC 3: in this case the chemocline was located right at the SWI (sea-water interface), oxygen values above the RPD where probably around the quasi anaerobic/dysaerobic boundary (0.1 to 0.2 ml L^{-1}).

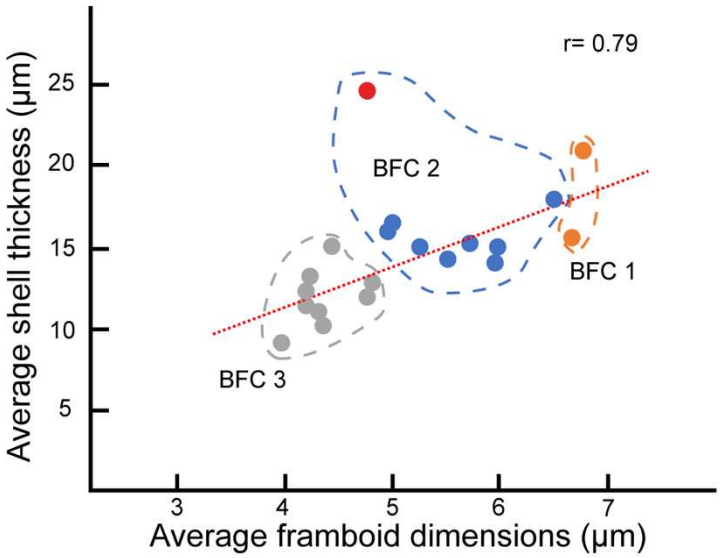

Fig. 10- Plot showing the distribution of framboidal pyrite vs average shell thickness for *Halobia cordillerana* at Tsiko Lake. The correlation coefficient has been calculated without the sample VI 68 A 2 (red dot): this sample gave anomalously high average shell thickness probably due to the fact that in this sample the valves' orientation is particularly affected by microbioturbation, thus biasing the measurement.